



ISSN: 0976-3031

Available Online at <http://www.recentscientific.com>

International Journal of Recent Scientific Research
Vol. 7, Issue, 12, pp. 14751-14754, December, 2016

**International Journal of
Recent Scientific
Research**

Research Article

OPTICAL BEHAVIOUR OF YTTRIUM DOPED MAGNESIUM-CADMIUM FERRITE PREPARED BY SOL-GEL AUTOCOMBUSTION METHOD

Bhise, R.B^{1,2} and Rathod S.M³

¹Department of Physics, B. J. College, Ale, Tal: Junnar, Dist: Pune, 412411, India

²Science College, SRTM University, Nanded, India

³Nanomaterials and Laser Research Laboratory, Abasaheb Garware College, Pune, 411004, India

ARTICLE INFO

Article History:

Received 16th September, 2016

Received in revised form 25th

October, 2016

Accepted 23rd November, 2016

Published online 28th December, 2016

Key Words:

Sol-gel Autocombustion Method, Ferrite Nanoparticles, Optical properties, XRD,

ABSTRACT

The present work represents, the Yttrium doped $Mg_{1-x}Cd_xY_yFe_{2-y}O_4$ (where $x = 0, 0.2, 0.4, 0.6$ and $y = 0, 0.075$) synthesized using sol-gel autocombustion method. The investigation of structural and optical properties was carried out for the synthesized samples using X-ray diffraction (XRD), Fourier transform infrared spectroscopy (FTIR) and Ultraviolet visible spectrophotometer (UV-Vis). XRD revealed that the structure of these nanoparticles is spinel with average grain size lies in the range between 17.79 to 24.2 nm. Lattice parameter was found to increase with Mg-Cd concentration and this may be due to the larger ionic radius of the Y^{3+} ion. FTIR spectroscopy confirmed the formation of spinel ferrite and showed the characteristic absorption bands around 477, 558, 1060, 1381, 1628, 1707, 2918, 3433 and 3841 cm^{-1} . The energy band gap was calculated for samples with different ratio and average band gap energy was found to be 4.2851 eV. The substitution was resulted in slight increase in the lattice constant and that sequentially may lead to the slightly increased in the energy gap. Also found that it is in the range of semiconductor materials.

Copyright © Bhise, R.B and Rathod S.M., 2016, this is an open-access article distributed under the terms of the Creative Commons Attribution License, which permits unrestricted use, distribution and reproduction in any medium, provided the original work is properly cited.

INTRODUCTION

Nanotechnology is one of the leading scientific fields today since it combines knowledge from the fields of Physics, Chemistry, Biology, Medicine and Engineering. The application and use of nanomaterials are extensive such as in electronic and mechanical devices, optical magnetic components, tissue engineering magnetic storage systems and magnetic resonance imaging [1-2]. Nanotechnology and material technology are new techniques for synthesis and processing manipulation and assembly using nature's own building blocks (atoms, molecules or macromolecules) for the intelligent design of functional materials, components and systems with attractive qualities and functions [3-4]. Ferrites are well-known magnetic nanomaterials intensively studied as a recording media due to their superior physical properties. These properties make ferrites an ideal candidate for technical applications such as magnetic resonance imaging enhancement, catalysis, sensors and pigments [5]. Mixed spinel ferrites have been studied intensively over the last few years due to their potential applications. Spinel ferrites have the chemical formula MFe_2O_4 in which M can be any divalent metal cations. In spinel ferrite, oxygen forms face centre cubic (FCC) lattice with divalent cations at tetrahedral (A) and/or octahedral (B)

sites. Magnesium ferrite ($MgFe_2O_4$) has an inverse spinel structure with the preference of Mg^{2+} cations mainly on octahedral sites [6-9], while Zinc ferrite ($ZnFe_2O_4$) has normal spinel structure, in which Zn^{2+} cations mainly occupy tetrahedral sites [6-10]. The small scale size of the well-known spinel ferrites has opened up the door for intensive research to utilize their properties for biomedical applications [11-13]. Numerous methods were reported in literature showing the possibilities of producing particle size in the range of 2 - 100 nm. Among these methods are co-precipitation, hydrothermal and sol-gel methods [14-15], which were reported to be fast and producing high quality nanoparticles.

In this work, $Mg_{1-x}Cd_xY_yFe_{2-y}O_4$ (where $x = 0, 0.2, 0.4, 0.6$ and $y = 0, 0.075$) were synthesized using co-precipitation methods. X-ray diffraction (XRD) was used in order to investigate the structural of Y^{3+} substituted magnesium-cadmium nano-ferrites and to determine the lattice parameters and the space group symmetry. Ultraviolet visible spectrometer (UV-Vis) and Fourier Transform Infrared Spectroscopy (FTIR) were used to investigate the optical properties of crystallite nanoparticles.

*Corresponding author: **Bhise, R.B**

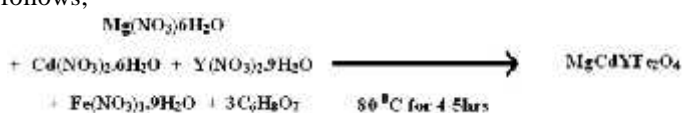
Department of Physics, B. J. College, Ale, Tal: Junnar, Dist: Pune, 412411, India

MATERIAL AND METHOD

The Y³⁺ doped in Mg-Cd ferrite powders were synthesized by sol-gel autocombustion method at low temperatures for different compositions of Mg_{1-x} Cd_x Y_y Fe_{2-y} O₄ (where x = 0, 0.2, 0.4, 0.6 and y = 0, 0.075). The AR grade nitrate of Merck company (purity of 99%) are used in the experiments such as Yttrium nitrate (Y(NO₃).6H₂O), Magnesium nitrate (Mg(NO₃).6H₂O), Cadmium nitrate (Cd(NO₃).6H₂O), Ferric nitrate (Fe(NO₃).9H₂O). These nitrates and citric acid are using stoichiometric ratio proportion to obtain the final product and the citric acid (C₆H₈O₇) is used as a fuel in the ratio 1:3. The proportion of each reagent was defined according to its respective molar amounts [16]. All chemicals are dissolved in distilled water and were stirred till to obtain the homogeneous solution. To maintain pH equal to 7 by adding drop by drop ammonium hydroxide (NH₄OH) during the stirring process. This solution was stirred continuously with 80 °C for about 4-5 hours to obtain sol. After 4-5 hours, gel converts into ash and ash convert into powder. Finally get fine powder of Mg_{1-x} Cd_x Y_y Fe_{2-y} O₄ ferrite nanoparticles after auto combustion. The powder was sintered at 400 °C for 2 hours.

The structural characterization was done using XRD analysis. The X-ray diffractometer with Cu-K radiation of wavelength 1.5405 Å⁰ at 40 kV performed a scanning from 20 to 80 degree at a step size of 0.02 degree per second for each prepared sample and determined crystal structure, lattice parameter and crystallite size. The optical characteristics was studied using Fourier Transformation Infrared spectroscopy (FT-IR) of Bruker 3000 Hyperion microscope with vertex 80 single point detector performing images resolution ranging between 7500 to 450 cm⁻¹ and UV-Visible spectroscopy. Further investigations of the optical properties are under way to elucidate the effective role of inter particle interactions in these samples.

The general chemical reaction of the synthesis sample is as follows;



RESULTS AND DISCUSSION

Structural Studies

XRD analysis: The resulting powder Mg_{1-x} Cd_x Y_y Fe_{2-y} O₄ (where x = 0, 0.2, 0.4, 0.6 and y = 0, 0.075) nanocrystals were characterized by XRD pattern. The XRD pattern of sintered Y³⁺ doped the magnesium-cadmium ferrite nano crystals as shown in figure-1. Obtained XRD pattern and crystalline phases were identified and it conformed the formation of a homogeneous well-defined spinal cubic structure with put any impurity. The broad peaks in the XRD pattern indicate a fine particle nature of the particles. The particle size was determined using Scherer's formula,

$$t = \frac{0.9\lambda}{\beta \cos \theta} \dots\dots (1)$$

Where, λ = wavelength of X-ray used, θ = peak position and β = FWHM of the peak and it is corrected for instrumental broadening. The average particle sizes of nanoparticles are given in Table-1. The particle size decreases as the concentration of Y³⁺ increases. Lattice parameter obtained for

prepared sample is ranging between 8.3562 to 8.3667 Å⁰ and average grain size ranging between 17.79 to 24.2 nm. The deviation in lattice parameter can be attributed to the cations rearrangement in the nano sized prepared ferrites. Value of lattice constant for Mg-Cd doped Yttrium ferrite shows the expansion of unit cell with rare earth doping when compared with pure Yttrium ferrite. This is expected due to substitution of large ionic radius of Y³⁺ ions (0.9 Å⁰) with small ionic radius Fe³⁺ ions (0.645 Å⁰). This result in Y³⁺ substituted ferrites to have higher thermal stability relative to Mg-Cd ferrite.

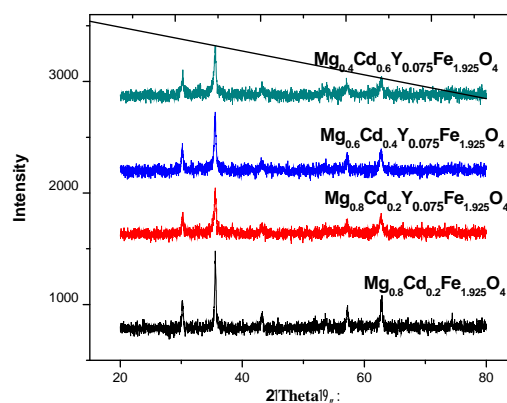


Figure 1 XRD pattern of Mg_{1-x} Cd_x Y_y Fe_{2-y} O₄

Table-1 The particle size of Mg_{1-x} Cd_x Y_y Fe_{2-y} O₄ by XRD

Obs. No.	Composition	Average grain size (t) nm	Lattice constant (a) Å ⁰
1	Mg _{0.8} Cd _{0.2} Fe ₂ O ₄	24.2	8.3601
2	Mg _{0.8} Cd _{0.2} Y _{0.075} Fe _{1.925} O ₄	23.24	8.3562
3	Mg _{0.6} Cd _{0.4} Y _{0.075} Fe _{1.925} O ₄	18.53	8.3667
4	Mg _{0.4} Cd _{0.6} Y _{0.075} Fe _{1.925} O ₄	17.79	8.3658

Optical studies

FT-IR Analysis: In order to investigate the chemical functional groups on the synthesized Mg_{1-x} Cd_x Y_y Fe_{2-y} O₄, FT-IR spectroscopy are performed. The FT-IR spectra of the prepared Mg_{0.6} Cd_{0.4} Y_{0.075} Fe_{1.925} O₄ are shown in figure 2 to know the bonding characteristics of the materials. The peaks at 477.53 cm⁻¹ and 558.79 cm⁻¹ are the peaks of Fe-O bond in Y doped Mg-Cd ferrite and it is arises due to the lattice vibrations of the oxide ions against cations. The peak at 1381.46 cm⁻¹ indicates the presence of O-H bond due to bending vibration. The broad peak at 3433.64 cm⁻¹ gives presence of hydroxyl group in the material and indicates that the material absorbed moisture from atmosphere during analysis.

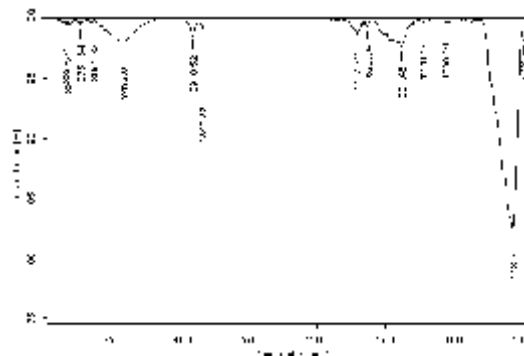


Figure 2a FT-IR spectrum of Mg_{0.6} Cd_{0.4} Y_{0.075} Fe_{1.925} O₄

The intense absorption bond is observed at 558.79 cm^{-1} which shows the characteristic bond of spinel structure which may due to presence of Fe-O and Y-O bonds or crystalline nature of Y doped Mg-Cd ferrite. Hence, FTIR analysis supports the observation of XRD analysis and confirms the crystalline nature of ferrite. So, the peaks at 417.17 cm^{-1} and 1060.24 cm^{-1} confirms the presence of yttrium doped in Mg-Cd ferrite. Finally, the doping of Y^{3+} on Mg-Cd ferrite was confirmed by different pattern of the plots and the difference in relative position and intensity of the peaks appeared in the FT-IR plots of the prepared samples.

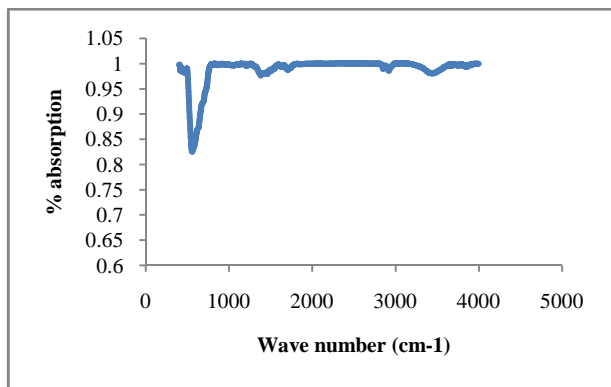


Figure 2 b Absorption spectra of $\text{Mg}_{0.6}\text{Cd}_{0.4}\text{Y}_{0.075}\text{Fe}_{1.925}\text{O}_4$

UV Visible Analysis: The figure 3 shows optical properties were studied from UV-Visible spectroscopy to calculate the band gap energy. In the absorption molecules of non-bonding electrons can absorb the energy in the form of ultraviolet or visible light to excite this electron to higher or anti-bonding molecular orbit. The energy band gap was calculated for samples with different ratio using following formula;

$$E = \frac{hc}{\lambda} \dots\dots (2)$$

Energy band gap was found to be 4.2538, 4.2980, 4.2906 and 4.2980 eV. The substitution was resulted in slight increase in the lattice constant and that sequentially may lead to the slightly decrease in the energy gap. The average Band gap of prepared sample is 4.2851 eV and wavelength absorb by 547.75 nm. It is in the range of semiconductor materials.

Table-2 The band gap energy of $\text{Mg}_{1-x}\text{Cd}_x\text{Y}_y\text{Fe}_{2-y}\text{O}_4$ by UV-Visible spectroscopy

Obs. No.	Composition	Wavelength (nm)	Band gap energy (eV)
1	x=0.2, y=0	291.5	4.2538
2	x=0.2, y=0.075	288.5	4.2980
3	x=0.4, y=0.075	289.0	4.2906
4	x=0.6, y=0.075	288.5	4.2980

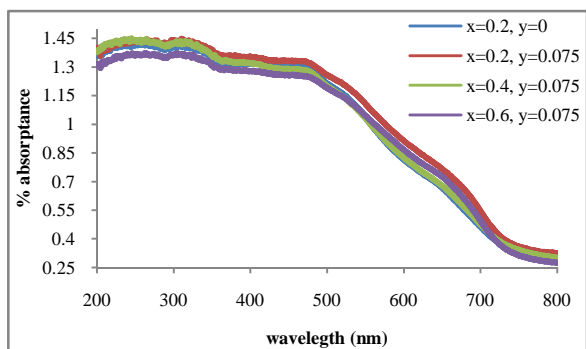


Figure 3 UV-Visible spectra of $\text{Mg}_{1-x}\text{Cd}_x\text{Y}_y\text{Fe}_{2-y}\text{O}_4$

CONCLUSION

The $\text{Mg}_{1-x}\text{Cd}_x\text{Y}_y\text{Fe}_{2-y}\text{O}_4$ nanoferrites were synthesized using sol-gel autocombustion technique. The increase in the Y^{3+} concentration gives the significant changes in the particle size and magnetic properties of the composition $\text{Mg}_{1-x}\text{Cd}_x\text{Y}_y\text{Fe}_{2-y}\text{O}_4$ (where $x = 0, 0.2, 0.4, 0.6$ and $y = 0, 0.075$). The FT-IR spectroscopy study shows two main metal oxygen bands in the range of 8.3562 to 8.3667 cm^{-1} confirming the formation of cubic spinel phase structure of Y^{3+} substitute in Ni-Cd ferrite. The synthesis of nanoparticles with crystalline size decreases and lattice constant increases as the concentration increases and is in the range of 17.79 to 24.2 nm for $400\text{ }^\circ\text{C}$. The UV-Visible analysis shows band gap energy increases with increase in Y^{3+} concentration. The UV-Visible study shows average Band gap energy is 4.2851 eV and wavelength absorb by 547.75 nm . It is in the range of semiconductor materials. So that synthesized samples is in the nature of semiconductor materials.

Acknowledgements

The authors are thankful to IIT, Powai (Mumbai), Savitribai Phule Pune University, Abasaheb Garware, College, Pune and PDE's Baburaoji Gholap College, New Sangavi, Pune, India for providing the instrumental facilities for the characterization purpose.

References

1. Flores-Acosta, M., Sotelo-Lerma, M., Arizpe-Chavez, H., Castillon-Barraza, F.F. and Ramirez-Bon, R.J. (2003) Excitonic Absorption of Spherical PbS Nanoparticles in Zeolite A. *Solid State Communications*, 128, 407-411. <http://dx.doi.org/10.1016/j.ssc.2003.09.008>
2. Pulisova, P., Kovac, J., Voigtd, A. and Raschman, P. (2013) Structure and Magnetic Properties of Co and Ni Nano-Ferrites Prepared by a Two Step Direct Microemulsions Synthesis. *Journal of Magnetism and Microemulsion Materials*, 341, 93-99. <http://dx.doi.org/10.1016/j.jmmm.2013.04.003>
3. Lodhi, M.Y., Mahmood, K., Mahmood, A., Malika, H., Warsi, M.F., Shakir, I., Asghar, M. and Khan, M.A. (2014) New $\text{Mg}_{0.5}\text{Co}_x\text{Zn}_{0.5-x}\text{Fe}_2\text{O}_4$ Nano-Ferrites: Structural Elucidation and Electromagnetic Behavior Evaluation. *Current Applied Physics*, 14, 716-720. <http://dx.doi.org/10.1016/j.cap.2014.02.021>
4. Jan, L.S., Radiman, S., Siddig, M.A., Muniandy, S.V., Hamid, M.A. and Jamali, H.D. (2004) Preparation of Nanoparticles of Polystyrene and Polyaniline by - Irradiation in Lyotropic Liquid Crystal. *Colloids and Surfaces A: Physicochemical and Engineering Aspects*, 251, 43-52. <http://dx.doi.org/10.1016/j.colsurfa.2004.09.025>
5. Mathew, D.S. and Juaug, R.-S. (2007) An Overview of the Structure and Magnetism of Spinel Ferrite Nanoparticles and Their Synthesis in Micro Emulsions. *Chemical Engineering Journal*, 129, 51-65. <http://dx.doi.org/10.1016/j.cej.2006.11.001>
6. Rahman, S., Nadeem, K., Anis-ur-Rehman, M., Mumtaz, M., Naeem, S. and Letofsky-Papst, I. (2013) Structural and Magnetic Properties of ZnMg-Ferrite Nanoparticles Prepared Using the Co-Precipitation

- Method. *Ceramics International*, 39, 5235-5239. <http://dx.doi.org/10.1016/j.ceramint.2012.12.023>
7. Pradeep, A., Priyadharsini, P. and Chandrasekaran, G. (2008) Sol-Gel Route of Synthesis of Nanoparticles of $MgFe_2O_4$ and XRD, FTIR and VSM Study. *Journal of Magnetism and Magnetic Materials*, 320, 2774-2779. <http://dx.doi.org/10.1016/j.jmmm.2008.06.012>
 8. Greenwood, N.N. and Earnshaw, A. (1984) Chemistry of the Elements; Pergamon Press Ltd., Oxford, 279.
 9. Ichiyanagi, Y., Kubota, M., Moritake, S., Kanazawa, Y., Yamada, T. and Uehashi, T. (2007) Magnetic Properties of Mg-Ferrite Nanoparticles. *Journal of Magnetism and Magnetic Materials*, 310, 2378-2380. <http://dx.doi.org/10.1016/j.jmmm.2006.10.737>
 10. Thummer, K.P., Chhantbar, M.C., Modi, K.B., Baldha, G.J. and Joshi, H.H. (2004) Localized Canted Spin Behaviour in $Zn_xMg_{1.5-x}Mn_{0.5}Fe_2O_4$ Spinel Ferrite System. *Journal of Magnetism and Magnetic Materials*, 280, 23-30. <http://dx.doi.org/10.1016/j.jmmm.2004.02.017>
 11. Kumara, C.S.S.R. and Mohammad, F. (2011) Magnetic Nanomaterials for Hyperthermia-Based Therapy and Controlled Drug Delivery. *Advanced Drug Delivery Reviews*, 63, 789-808. <http://dx.doi.org/10.1016/j.addr.2011.03.008>
 12. Giri, J., Pradhan, P., Somani, V., Chelawat, H., Chhatre, S., Banerjee, R. and Bahadur, D. (2008) Synthesis and Characterizations of Water-Based Ferrofluids of Substituted Ferrites [$Fe_{1-x}B_xFe_2O_4$, B=Mn, Co ($x=0-1$)] for Biomedical Applications. *Journal of Magnetism and Magnetic Materials*, 320, 724-730. <http://dx.doi.org/10.1016/j.jmmm.2007.08.010>
 13. Sharifi, I., Shokrollahi, H. and Amiri, S. (2012) Ferrite-Based Magnetic Nanofluids Used in Hyperthermia Applications. *Journal of Magnetism and Magnetic Materials*, 324, 903-915. <http://dx.doi.org/10.1016/j.jmmm.2011.10.017>
 14. Chen, Y., Ruan, M., Jiang, Y.F., Cheng, S.G. and Li, W. (2010) The Synthesis and Thermal Effect of $CoFe_2O_4$ Nanoparticles. *Journal of Alloys and Compounds*, 493, L36-L38. <http://dx.doi.org/10.1016/j.jallcom.2009.12.170>
 15. Liu, Q., Sun, J.H., Long, H.R., Sun, X.Q., Zhong, X.J. and Xu, Z. (2008) Hydrothermal Synthesis of $CoFe_2O_4$ Nanoplatelets and Nanoparticles. *Materials Chemistry and Physics*, 108, 269-273. <http://dx.doi.org/10.1016/j.matchemphys.2007.09.035>
 16. Bhise, R.B. and Rathod, S.M. June (2016) Synthesis of Nanosized Y^{3+} Doped Ni-Mg-Cd Ferrite Powders and their Structural, Magnetic properties by Sol-gel Auto Combustion Method. *Res. J. Material Sci.*, Vol. 4(5), 1-4. E-ISSN 2320-6055

How to cite this article:

Bhise, R.B and Rathod S.M.2016, Optical Behaviour of Yttrium Doped Magnesium-Cadmium Ferrite Prepared By Sol-Gel Autocombustion Method. *Int J Recent Sci Res.* 7(12), pp. 14751-14754.